CONFIDENTIAL

Copy 94
RM L52L09

NACA

RESEARCH MEMORANDUM

WING AND FUSELAGE LOADS MEASURED IN FLIGHT ON THE NORTH AMERICAN B-45 AND F-82 AIRPLANES

By Paul W. Harper

Langley Aeronautical Laboratory
Langley Field, Va.

CLASSIFIED DOCUMENT

This material contains information affecting the National Defense of the United States within the meaning of the espionage laws, Title 18, U.S.C. Secs. 793 and 794, the transmission or revelation of which in any manner to an unauthorized person is prohibited by law.

NATIONAL ADVISORY COMMITTEE
FOR AERONAUTICS

WASHINGTON

February 2, 1953

CONFIDENTIAL

NATIONAL ADVISORY COMMITTEE FOR AERONAUTICS

RESEARCH MEMORANDUM

WING AND FUSELAGE LOADS MEASURED IN FLIGHT ON THE NORTH AMERICAN B-45 AND F-82 AIRPLANES

By Paul W. Harper

SUMMARY

Flight investigations were conducted to determine the wing and fuselage loads on the North American B-45 and F-82 airplanes by means of calibrated strain-gage installations at each wing- and tail-fuselage juncture. The tests covered a Mach number range of approximately 0.3 to 0.75 and a normal-force-coefficient range from about -0.5 to 1.0. For the F-82 airplane data were obtained for various power settings from zero to full power.

The aerodynamic loads measured on the B-45 airplane were substantially as predicted by theory. The wing-fuselage division of the load was constant over the test ranges of Mach number and normal-force coefficient. A small outboard shift of wing center of pressure with increasing Mach number was indicated.

For the F-82 airplane the fraction of the total additional air load carried by the exposed wings was approximately 10 percent less than that predicted by theory, and the load on the fuselages proportionately larger. The division-of-load and center-of-pressure results indicated a gradual outboard shift of fuselage and outer-wing loads with increasing Mach number. The effect of power on the division of load appeared to be negligible.

INTRODUCTION

The trend toward higher speeds, thinner wings, and larger ratios of fuselage diameter to wing span has extended interest in the general wing-fuselage interference problem to the division of the total load between the wing and the fuselage. The status of the experimental portion of the loads phase is included in reference 1, which presents a collection of data on the division of load between wing and fuselage as obtained from wind-tunnel and rocket-propelled tests and from flight tests on several present-day airplanes. The results indicate that the fuselage carries a load nearly proportional to the area of the wing blanketed by the

fuselage. A procedure for predicting the division of load on a wing-body combination is given in reference 2. Predictions made by this method were shown to be in good agreement with results of wind-tunnel tests on three wing-body combinations having large ratios of body diameter to wing span and low-aspect-ratio wings.

In order to supplement the available information on the division of load between wing and fuselage, this paper presents the loads and bending moments measured in flight over the Mach number range from 0.30 to 0.75 on a high-wing airplane with wing nacelles, the North American B-45, and an unconventional twin-fuselage low-wing airplane, the North American F-82.

SYMBOLS

W	airplane weight, lb
W_c	component weight, lb
W_c'	value of W_c during ground-reference measurement
A	total wing area including that intercepted by fuselage, ft^2
b	wing span, in.
y	lateral distance from airplane center line, in.
y_g	value of y at gage station, in.
g	acceleration due to gravity, ft/sec^2
q	dynamic pressure, lb/sq ft
n	airplane normal load factor at airplane center of gravity, g units
Δn	increment in normal acceleration at the center of gravity of a component due to angular accelerations, g units
M	Mach number
C_{N_W}	normal-force coefficient of exposed wing
C_{N_c}	normal-force coefficient of component, L_c/qA
$C_{N_{c_o}}$	normal-force coefficient of component when $C_{N_{WF}} = 0$

$C_{N_{WF}}$ normal-force coefficient of wing-fuselage combination

L total airplane lift, $\sum L_c$, lb

L_c aerodynamic load on component, lb

L_{c_o} aerodynamic load on component when $C_{N_{WF}} = 0$, lb

S_a aerodynamic shear at strain-gage station, lb

S structural shear at strain-gage station, lb

BM aerodynamic bending moment at strain-gage station, in-lb

BM_o aerodynamic bending moment at strain-gage station when $S_a = 0$, in-lb

$\bar{y}$ rate of change of air-load moment with air-load shear at pertinent gage station, in.

R reaction of right or left landing gear on airplane structure at time of ground-reference measurements, lb

APPARATUS AND TESTS

Three-view drawings of the test airplanes are shown in figures 1 and 2, and the principal physical characteristics are listed in table I. The B-45 is a high-wing, jet-propelled, medium bomber having two wing nacelles. The F-82 is a low-wing, twin-fuselage airplane with counter-rotating propellers.

Instrumentation.- The instrumentation of both airplanes was similar insofar as the subject tests were concerned. Standard NACA recording instruments were used for measuring airspeed, altitude, dynamic pressure, normal acceleration at the airplane center of gravity and the horizontal tail, pitching acceleration, and control position. Multichannel oscillographs were used for recording strain-gage outputs.

Strain gages were installed at each wing- and tail-fuselage juncture for measuring shear and bending moment. Thus there were four strain-gage stations on the B-45 and six gage stations on the F-82, as shown in figures 1 and 2. Gages were mounted as close as practical to the fuselages. The spanwise locations of the gage stations are listed in table I.

Calibration of the gages on the B-45 was made by supporting the airplane from the fuselage with the landing gear retracted and applying

numerous point loads to wing and tail surfaces in the manner described in reference 3. These loads, of various magnitudes up to 3,000 pounds, were each applied through a pad of sufficient size so as not to cause local failures. Gages were then electrically combined to eliminate torque effects. From the calibrations, equations for shear and for moment at each gage station were derived of the form

$$\left.\begin{aligned} \text{Shear} &= A_s\delta_s + B_s\delta_m \\ \text{Moment} &= A_m\delta_s + B_m\delta_m \end{aligned}\right\} \qquad (1)$$

where the δ's are the deflections of the combined-gage circuit outputs and A and B are the calibration constants. Following the procedure of reference 3 the least-squares determination of the constants in equations (1) indicated probable errors of 50 pounds and 10,000 inch-pounds in computing the gage-station shears and moments due to any of the applied calibration loads.

Calibration of the gages on the F-82 was similarly obtained. In this case because of its peculiar configuration the airplane was supported during calibration by an overhead linkage system and fuselage slings in such a manner as not to impart restraint to the flow of shear and moment across the fuselage. With the system of support used, the fuselages were free to twist and pitch with respect to each other. Point and distributed calibration loadings of magnitudes ranging from 250 to 3,000 pounds were applied to all lifting panels. The probable errors (obtained similarly to those for the B-45) for computing shear or moment at any of the four wing gage stations were 50 pounds and 4,000 inch-pounds.

Tests.- Conditions of the flight tests for both airplanes are summarized in tables II and III. Maneuvers covering a range of load factor below the stall and consisting of wind-up turns and push-down pull-ups (push-pulls) were made at various Mach numbers covering a range of about 0.3 to 0.75. Mach number and dynamic pressure were held practically constant during any given run, and yawing and rolling were held to a minimum. Aileron-position variations averaged less than $\pm 1/2^{\circ}$.

The tests on the B-45 consisted of a series of runs at each of several altitudes from 15,000 to 30,000 feet. No attempt was made to control or vary the power in any specified manner. The push-down pull-ups were classified as abrupt.

For the F-82 all runs were made at an altitude near 16,000 feet. Several series of runs were made at different Mach numbers with manifold pressure and engine speed held constant. Another series was made at various manifold pressures from idling to maximum power with engine speed

constant and Mach number constant at about 0.5. Several runs were made with one propeller feathered and the other engine at normal rated power. The remaining runs were made with no power conditions specified. The push-down pull-ups were classed as medium fast except for two runs in which pitching acceleration was made as large as practical for the purpose of determining the pitching moment of inertia about the Y-axis.

METHOD

In order that the data may be better interpreted, a brief review of the procedure used in reducing the loads measurements is given.

The shear load on a wing of the B-45 airplane can be used for an illustrative case. The structural shear S at the root gage station was equated to the summation of the normal forces acting outboard of the station with a ground zero used as a reference condition. On the ground the relation between the various factors is

$$S_{grd} = (R - W_c') \tag{2}$$

while in flight the corresponding relation is

$$S_{flt} = L_c - nW_c \tag{3}$$

where the component weight W_c includes a variable fuel weight which can be estimated with good accuracy from fuel-consumption measurements. Therefore with the ground zero as a reference condition the air load L_c can be determined from

$$S = S_{flt} - S_{grd} = L_c - nW_c - (R - W_c') \tag{4}$$

where the terms in parentheses are constants for any given flight, R is obtained with weighing capsules, and the structural shear S is obtained from the strain-gage equations.

Evaluation of the air-load moments was governed by a similar procedure in which the shear terms in equation (4) are replaced by equivalent moment terms.

Although the load equation for a B-45 wing was used to illustrate the procedure, the equations for the F-82 are relatively more involved because of the greater number of components; therefore to show the

relations among the various component loadings and the total airplane lift, the F-82 loads equations are summarized below. A diagrammatic sketch and appropriate subscripts are used to identify locations of the quantities considered.

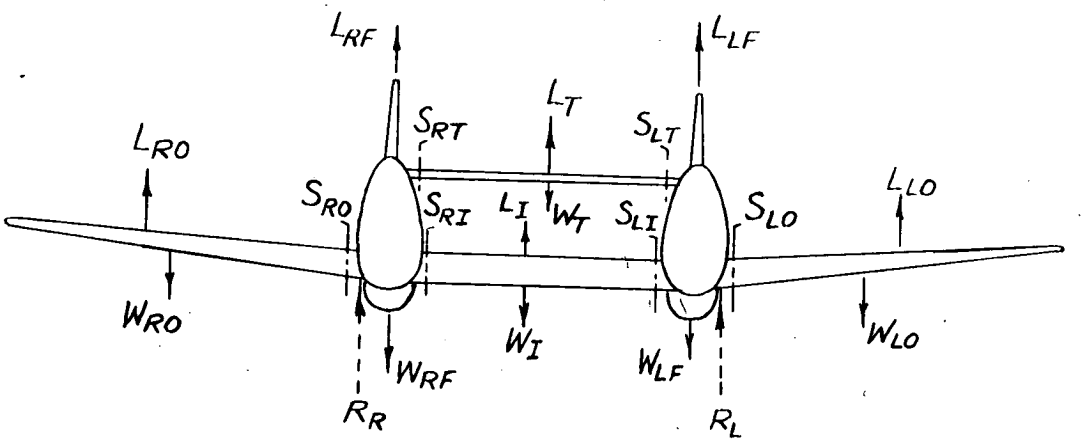

$$\left(\begin{matrix}\text{Component}\\ \text{air load}\end{matrix}\right) = \left(\begin{matrix}\text{Component}\\ \text{structural shear}\\ \text{load}\end{matrix}\right) + \left(\begin{matrix}\text{Component}\\ \text{flight inertia load}\end{matrix}\right) - \left(\begin{matrix}\text{Ground-}\\ \text{reference}\\ \text{load}\end{matrix}\right)$$

$$L_{LO} = \left(S_{LO} - 0\right) + \left(W_{LO}\right)\left(n + \Delta n_{LO}\right) - \left(W'_{LO}\right)$$

$$L_{RO} = \left(S_{RO} - 0\right) + \left(W_{RO}\right)\left(n + \Delta n_{RO}\right) - \left(W'_{RO}\right)$$

$$L_I = -\left(S_{LI} + S_{RI}\right) + \left(W_I\right)\left(n + \Delta n_I\right) - \left(W'_I\right)$$

$$L_{LF} = \left(S_{LI} + S_{LT} - S_{LO}\right) + \left(W_{LF}\right)\left(n + \Delta n_{LF}\right) - \left(W'_{LF} - R_L\right)$$

$$L_{RF} = \left(S_{RI} + S_{RT} - S_{RO}\right) + \left(W_{RF}\right)\left(n + \Delta n_{RF}\right) - \left(W'_{RF} - R_R\right)$$

$$L_T = -\left(S_{LT} + S_{RT}\right) + \left(W_T\right)\left(n + \Delta n_T\right) - \left(W'_T\right)$$

$$L = \sum L_c = 0 + (W)n - 0$$

$$L_{WF} = nW - L_T = \sum(\text{wing and fuselage load components})$$

The structural-shear term represents the instantaneous difference between structural shears measured at the two sides of the component under consideration. The Δn terms were negligible in nearly all maneuvers except for the case of the tail component where it was necessary to include the effects of pitching.

Time histories of wing moments and component air loads of the B-45 and the F-82 were evaluated for each maneuver. Since the boundaries of a component are defined by the strain-gage stations, the computed fuselage loads include the total load between gage stations at either side. The fuel loads (and therefore component weights) were assumed constant during a particular maneuver.

The method of presentation of results follows the concept that the lift or load distribution over a wing is usually considered to consist of a basic distribution plus an additional distribution. The basic load has a net lift of zero and for a given dynamic pressure is a function of wing geometry, elastic twist, aileron deflection, and rate of roll but is independent of angle of attack. The additional distribution, for a given plan form, depends only on angle of attack or normal-force coefficient at a given Mach number and dynamic pressure.

The estimated maximum fixed errors expected for the principal measured and evaluated quantities are listed in table IV. These are based on instrument and gage calibration errors, knowledge of the airplane weight distribution, and determination of ground-reference loads. The net effect of random errors due to reading records and so forth will be evident from scatter of the flight data to be presented.

For comparison with experimental results, theoretical values were computed for component additional loading and additional centers of pressure in accordance with current design practice (as in ref. 1). Thus for a wing-body combination an equivalent wing is assumed for which the portion of span intercepted by the body is replaced by wing sections formed by extending the exposed-wing leading and trailing edges to the body center line.

The spanwise additional load distribution for this equivalent wing was computed by using incompressible lifting-line theory. Centers of pressure were computed for this load distribution and estimated load ratios were obtained as the ratio of the area under the load-distribution curve between any two span stations to the total area under the curve. This procedure will be referred to as wing theory.

Estimated load ratios were also obtained by using the concepts presented in reference 2 and these will be referred to as "wing-body theory." In reference 2, the exposed-wing loading is obtained from theoretical considerations (including the effects of body induction); the intercepted wing load is considered to be a function of the exposed wing load and the ratio of body diameter to wing span as given by the Lennertz load carryover factor; the afterbody normal load is considered negligible; and the forebody load is computed from potential flow relations given by Multhopp. For the B-45 airplane the forebody load on the nacelles was also considered. Since the F-82 configuration included two fuselages,

the equivalent Lennertz load carry-over for this airplane was arbitrarily assumed to be double that computed for one fuselage.

RESULTS AND DISCUSSION

B-45 Airplane

Component loading.- The variations of the component normal-force coefficients C_{N_c} with wing-fuselage normal-force coefficient $C_{N_{WF}}$ during a typical wind-up turning maneuver and during a typical push-pull maneuver are plotted in figure 3. Curves are drawn through the points for left wing and for the fuselage. It is worth noting that in a plot of this kind the relations of the component loadings to each other and to $C_{N_{WF}}$ (airplane-less-tail load coefficient) are independent of tail loads. The variations are seen to be linear with $C_{N_{WF}}$ throughout the range of the maneuvers and can be represented by the equation

$$C_{N_c} = \frac{dC_{N_c}}{dC_{N_{WF}}} C_{N_{WF}} + C_{N_{c_o}} \tag{5}$$

where $\frac{dC_{N_c}}{dC_{N_{WF}}}$ gives the fractional part of the additional wing-fuselage load which acts on the components, and the intercept $C_{N_{c_o}}$ represents the loading on the component when $C_{N_{WF}}$ equals zero. In figure 3, values of $\frac{dC_{N_c}}{dC_{N_{WF}}}$ and $C_{N_{c_o}}$ are tabulated for the runs plotted. It is seen that the summation of the $\frac{dC_{N_c}}{dC_{N_{WF}}}$ values should equal one, and that the summation of the $C_{N_{c_o}}$ values should equal zero.

For each component in each run a least-squares solution for $\frac{dC_{N_c}}{dC_{N_{WF}}}$ and $C_{N_{c_o}}$ was made and the results are shown in figures 4 and 5.

In figure 4 the variation of the additional air-load division with Mach number at several altitudes is presented and compared with estimated values. The two theoretical methods give about the same load ratio and are in good agreement with experimental values. The ratios of the

CONFIDENTIAL

component areas (table I) to the total wing area are nearly identical to the theoretical values and thus also give a good approximation of the division of load. There is no apparent change in load division with either Mach number or altitude. Somewhat more scatter is apparent for the points obtained from turns at 15,000 and 30,000 feet than for the push-pulls at 20,000 feet because of the limited C_N range available for computing slopes, as indicated in figure 3 and table II.

Figure 5 gives the variation of component air load at zero lift with dynamic pressure for various altitudes and maneuvers. No consistent variation with altitude is indicated. With the exception of flight 11 the mean level of the values for each component is within the estimated error (table IV), does not change with q, and is therefore probably due to errors in computation of ground-reference loads. It is believed then that the component loads are approximately zero at zero lift. In view of the lack of knowledge of the aeroelastic properties of the wing (measurements of wing twist due to air load, etc.) and zero-lift characteristics of the fuselage and nacelles, no estimated values for basic load division can be given.

Wing moments.- The air-load moments measured at the right gage station are plotted in figure 6 against the right-wing air-load shear measured during a typical turn and during a typical push-pull maneuver. The variations, which are linear throughout the range of measurement, may be represented by the equation

$$BM = \frac{dBM}{dS_a} S_a + BM_o \tag{6}$$

where dBM/dS_a is the additional air-load center of pressure in inches measured from the gage station, and BM_o (a function of q) is the air-load moment when S_a equals zero. Here q and therefore BM_o was assumed constant during a run. As in the case of the load a least-squares evaluation of the data was made for each run and the results are plotted in figures 7 and 8.

Figure 7 shows the additional air-load center-of-pressure variation with Mach number for several altitudes. The values are presented as fractions of that portion of the span outboard of the gage station. Any variation with altitude and Mach number is effectively masked by the relatively large scatter for the turn data. The more consistent push-pull data show a gradual outboard shift in center-of-pressure position with Mach number of about 4 percent. The agreement of the average of the values with the theoretical value is good.

Figure 8 shows the zero-lift air-load moments plotted against q where it is seen that BM_o appears to be a function of additional variables and not a simple linear function of q as would be expected for a rigid structure. For instance, the BM_o values given for a constant altitude of 20,000 feet appear constant with dynamic pressure.

Since the preceding method of analysis (figs. 7 and 8) failed to account for the scatter in the bending-moment data, the degree of dependence of the measured bending moment on a number of additional measured variables was investigated by adding additional terms in various combinations to equation (6) and by using selected data from each run in each flight combined simultaneously to obtain a better correlation. In each case the constants were evaluated from a set of N simultaneous equations, each of which contained particular values of the independent variables from a particular run. Since two sets of values per run were used (corresponding to the maximum and minimum values of BM in each run as computed by eq. (6)) N was equal to 2(Total number of runs). The number of equations was reduced to the number of unknowns by the usual least-squares normalizing procedure. It is evident that errors in determining the constants in equation (6) for only one run and a limited range of the variables are minimized in the procedure which utilized all the data simultaneously.

The best representation of the data, based on theory of least-squares criteria, was given by

Left wing:

$$BM = (194.0 \pm 0.4)S_a + (700 \pm 70)q + (5900 \pm 300)\Delta T$$

Right wing:

$$BM = (193.8 \pm 0.3)S_a + (680 \pm 50)q + (2900 \pm 200)\Delta T \qquad (7)$$

where the first two terms are the same as in equation (6) except for the consideration of a variable q, and ΔT is the airplane structure temperature during ground-reference measurements minus the temperature during the particular maneuver in flight.

The degree to which equations (7) represent the measured moment during a typical maneuver is illustrated graphically in figure 9 where a time-history comparison is made between the measured bending moment and the bending moment computed from measured values of S_a, q, and ΔT during the maneuver. The degree to which equations (7) represent all the flight data is indicated numerically by the probable errors included in the parentheses for each of the coefficients (obtained as a by-product of the least-squares solution) from which the probable error in BM was

obtained as less than 50,000 inch-pounds. The center-of-pressure value of 194 inches in equation (7) is equivalent to 0.419 in nondimensional units which agrees well with the theoretical value 0.421 given in figure 7. A considerable degree of confidence is indicated for the coefficient of q when it is noted that, notwithstanding its small magnitude, the values for the right and left sides were nearly identical.

Equations (7) explicitly give bending moment as measured. If the temperature term is assumed to indicate a fictitious bending moment, then the actual wing bending moments are the measured values corrected for temperature effect by rearranging equations (7) as follows:

$$BM_{actual} = BM_{meas} - C_3\Delta T = C_1 S_a + C_2 q \tag{8}$$

where C_1, C_2, and C_3 are the constants in equations (7).

The type of treatment given the bending-moment data was not warranted for the division of load data because of the small magnitude of the component loadings at zero lift.

F-82 Airplane

Component loading.- The division of the load between left wing, inner wing, and left fuselage as a function of wing-fuselage normal-force coefficient during a typical push-pull maneuver of the F-82 airplane is plotted in figure 10. The right-wing and right-fuselage force coefficients were omitted for clarity since the variation and magnitude of these values were similar to those shown for the left wing and fuselage. The dependence is noted to be linear throughout the range of $C_{N_{WF}}$. Treatment of the data for each maneuver was made similarly to that for the B-45 and the results are presented in figures 11, 12, and 13.

In figure 11 the additional air-load division at several Mach numbers is compared with theoretical values. Above a Mach number of 0.5 the outer-wing load increases and the fuselage loads decrease with increasing Mach number. The fraction of the load carried by the inner wing remains essentially constant. The load carried by the total exposed wing is approximately 10 percent less than predicted by theory and that on the fuselages is proportionately higher. The disagreement is slightly less when compared to the wing-body theory but is generally larger than would be expected due to experimental error. As in the case of the B-45 the wing-area ratios are in agreement with the theoretical values and thus in disagreement with experimental values.

Since the configuration of the F-82 airplane is somewhat unusual, it is probable that somewhat greater reliance can be placed on the outer-wing-load measurement than on those of the inner wing and fuselage.

It is of interest to comment that qualitatively the disagreement with theory of the outer-wing-load component was noted to be the same as that measured for the North American F-51D airplane (ref. 1) which has a configuration very similar to that of the F-82 airplane outboard of the fuselage vertical planes of symmetry. For the F-51D the experimental exposed-wing load ratio was 0.76, that by wing theory 0.80, and that by wing-body theory of reference 2 was 0.78.

The better correlation with the theoretical values shown by the B-45 experimental results could be attributed to the additional load contributed to the exposed wing by the nacelles. The other principal dissimilarity between the B-45 and the F-82 (and the F-51D) is the vertical location of the wing-body intersections.

Figure 12 gives the variation of component air load at zero lift, L_{c_0}, with dynamic pressure. The scatter is necessarily large because the magnitude of the loads approaches the measurement-error magnitude and no attempt was made to draw curves. The inner-wing load increases negatively with q in a somewhat linear manner and the outer-wing loads increase positively. The values for the outer-wing loads should be shifted so as to extrapolate through zero at zero q, indicating the likelihood of errors in determination of ground-reference loads. This shift of the wing-load values would automatically shift the fuselage-load values toward zero, which would explain the lack of change with q shown by the fuselage-load plots. Since the incidence of the fuselages and outer wings is negative with respect to the inner wing, it would appear that the signs of the loads are opposite from that which would be expected. For reasons mentioned in connection with the B-45 zero-lift results no estimated zero-lift values can be given.

The effect of power on the F-82 load division is shown in figure 13 where manifold pressure, used as the criterion of power, is varied from the idling condition to the full-power condition. The additional load division is given at the bottom of figure 13 and the zero-lift division at the top in terms of component normal-force coefficient. The effect of asymmetrical power is also shown for the condition of propeller feathered and power off on one engine and normal rated power (50 in. Hg) on the other. An apparent lack of any significant power effect is indicated in figure 13 although some effect of power might be expected due to thrust, slipstream, and related factors. Since the area swept by the slipstreams includes a portion of each wing as well as the fuselages, it can be inferred that either the power affects the components proportionately or the effects on the span loading are negligible.

Wing moments.- Plots of aerodynamic bending moment as a function of aerodynamic shear at the four gage stations on the F-82 were typically as shown in figure 6 for the B-45 airplane. Results of evaluating centers of pressure and zero lift intercepts for each run are summarized in figures 14 and 15.

The effect of Mach number on the additional air-load centers of pressure is shown in figure 14. An outboard shift of load with increasing Mach number is indicated at both inner and outer stations. The greater amount of shift measured at the inner stations is in agreement with the shift in load from fuselage to wing noted in connection with figure 11. The center of pressure measured at the outer station for low Mach numbers is in fair agreement with the theoretical value. At the inner station the measured values are considerably less than the theoretical.

Bending moments at zero shear at the four stations are shown as a function of dynamic pressure in figure 15. As would be expected the zero-lift bending moment increases negatively with dynamic pressure, and within the experimental-error limits the values appear to be a linear function of q. It is seen that the values do not extrapolate to zero at zero q as expected. However, a shift of the zero-lift outer-wing loads, suggested previously in connection with figure 12, would have approximately eliminated the intercept discrepancy for the outer-gage-station results shown in figure 15.

SUMMARY OF RESULTS

The aerodynamic loads measured on the North American B-45 airplane were substantially as predicted by theory. The wing-fuselage division of the additional load was constant over the test ranges of Mach number and normal-force coefficient. A small outboard shift of wing center of pressure with increasing Mach number was indicated.

For the North American F-82 airplane the fraction of the total additional air load carried by the exposed wings was approximately 10 percent less than that predicted by theory, and the load on the fuselages was proportionately larger. The division-of-load and center-of-pressure results indicated a gradual outboard shift of fuselage and outer-wing loads with increasing Mach number. The effect of power on the division of load appeared to be negligible.

Langley Aeronautical Laboratory,
National Advisory Committee for Aeronautics,
Langley Field, Va.

REFERENCES

1. Mayer, John P., and Gillis, Clarence L.: Division of Load Among the Wing, Fuselage, and Tail of Aircraft. NACA RM L51E14a, 1951.

2. Hopkins, Edward J., and Carel, Hubert C.: Experimental and Theoretical Study of the Effects of Body Size on the Aerodynamic Characteristics of an Aspect Ratio 3.0 Wing-Body Combination. NACA RM A51G24, 1951.

3. Skopinski, T. H., Aiken, William S., Jr., and Huston, Wilber B.: Calibration of Strain-Gage Installations in Aircraft Structures for the Measurement of Flight Loads. NACA RM L52G31, 1952.

TABLE I.- PHYSICAL CHARACTERISTICS OF TEST AIRPLANES

	B-45	F-82
Wing:		
Span, ft	89.04	51.23
Mean aerodynamic chord, ft	14.02	8.22
Aspect ratio	6.74	6.42
Taper ratio (outer panel for F-82)	0.413	0.561
Wing trailing edge	Reflexed	------
Areas:		
Wing and intercepted fuselage, sq ft	1175	408.6
Intercepted fuselage (between gage sta.), sq ft	213	38.1 each
Inner wing (between gage sta.), sq ft	------	100.4
Outer wing (outboard from gage sta.), sq ft	962	116.1 each
Incidences:		
Inner wing, deg	------	0
Wing root, deg	0	0
Fuselage axis, deg	-3	-1.5
Wing tip, deg	-2.5	-3.5
Nacelles, deg	-3.0	------
Thrust axis, deg	-3.0	-3.25
Airplane weight, lb (average during tests)	59,000	18,600
Center of gravity, percent MAC	27	27
Strain-gage station:		
Inner, inches from airplane center line	------	64.4
Outer, inches from airplane center line	71	113
Tail, inches from airplane center line	18	72.3

TABLE II.- SUMMARY OF FLIGHT TEST CONDITIONS FOR THE B-45 AIRPLANE

Flight	Run	Maneuver	$C_{N_{WF}}$		Mach number	Dynamic pressure, lb/ft^2	Pressure altitude, ft
			Min.	Max.			
15	2	Turn	0.13	0.30	0.74	450	15,000
	3	Turn	.12	.37	.71	433	15,000
	4	Turn	.13	.37	.70	413	15,000
	5	Turn	.10	.37	.68	386	15,000
	6	Turn	.12	.41	.66	356	15,000
	7	Turn	.12	.43	.64	346	15,000
	8	Turn	.15	.45	.62	318	15,000
	9	Turn	.18	.48	.60	299	15,000
	10	Turn	.19	.50	.57	276	15,000
	11	Turn	.20	.58	.53	238	15,000
	12	Turn	.24	.62	.49	201	15,000
	13	Turn	.29	.65	.45	167	15,000
	14	Turn	.38	.71	.40	133	15,000
	15	Turn	.40	.76	.38	122	15,000
	16	Turn	.44	.78	.36	110	15,000
	17	Turn	.49	.80	.35	99	15,000
	18	Turn	.36	.68	.40	136	15,000
18	1	Push-pull	-.09	.38	.74	367	20,000
	2	Push-pull	-.11	.51	.72	358	20,000
	3	Push-pull	-.09	.45	.72	350	20,000
	4	Push-pull	-.09	.56	.71	338	20,000
	5	Push-pull	-.13	.44	.70	338	20,000
	6	Push-pull	-.10	.56	.67	307	20,000
	7	Push-pull	-.13	.55	.65	294	20,000
	8	Push-pull	-.15	.62	.62	262	20,000
	9	Push-pull	-.13	.72	.58	230	20,000
	10	Push-pull	-.18	.72	.54	197	20,000
	11	Push-pull	-.21	.82	.50	169	20,000
	12	Push-pull	-.26	.82	.45	134	20,000
	13	Push-pull	-.35	.92	.40	109	20,000
	14	Push-pull	-.41	1.11	.35	82	20,000
	15	Push-pull	-.23	.75	.55	206	20,000
	16	Push-pull	-.23	.62	.50	169	20,000

TABLE II.- SUMMARY OF FLIGHT TEST CONDITIONS FOR THE B-45 AIRPLANE - Concluded

Flight	Run	Maneuver	$C_{N_{WF}}$ Min.	$C_{N_{WF}}$ Max.	Mach number	Dynamic pressure, lb/ft^2	Approximate pressure altitude, ft
13	1	Turn	0.66	0.87	0.36	78	22,000
	2	Turn	.60	.92	.36	78	22,000
	3	Turn	.57	.88	.38	87	22,000
	4	Turn	.51	.85	.40	98	22,000
	5	Turn	.41	.79	.44	119	22,000
	6	Turn	.31	.71	.48	143	22,000
	7	Turn	.30	.69	.53	172	22,000
	8	Turn	.25	.68	.57	200	22,000
	9	Turn	.22	.61	.62	235	22,000
	10	Turn	.18	.54	.66	268	22,000
	11	Turn	.18	.49	.68	285	22,000
	12	Turn	.17	.39	.70	295	22,000
	13	Turn	.16	.26	.72	316	22,000
	14	Turn	.14	.21	.74	341	22,000
	15	Turn	.02	.17	.76	360	22,000
11	1	Turn	.81	.43	.38	66	30,000
	2	Turn	.66	.87	.42	78	30,000
	3	Turn	.56	.83	.45	91	30,000
	4	Turn	.50	.83	.48	102	30,000
	5	Turn	.44	.80	.51	115	30,000
	6	Turn	.38	.79	.55	129	30,000
	7	Turn	.32	.82	.58	149	30,000
	8	Turn	.31	.78	.61	162	30,000
	9	Turn	.29	.74	.65	186	30,000
	10	Turn	.26	.73	.68	202	30,000
	11	Turn	.23	.68	.70	211	30,000
	12	Turn	.22	.55	.72	223	30,000
	13	Turn	.22	.50	.74	242	30,000
	14	Turn	.18	.36	.76	262	30,000

TABLE III.- SUMMARY OF FLIGHT TEST CONDITIONS FOR THE F-82 AIRPLANE

Flight	Run	Maneuver	$C_{N_{WF}}$		Mach number	Dynamic pressure, lb/ft^2	Pressure altitude, ft	Engine manifold pressure, in. Hg.	
			Min.	Max.				Left	Right
4	1	Push-pull	0.00	0.61	0.71	409	16.0×10^3	46	46
	2	Push-pull	-.09	.62	.62	316	15.0	46	46
	3	Push-pull	-.22	.86	.52	209	16.0	46	46
	4	Push-pull	-.33	.95	.42	137	17.5	46	46
	5	Push-pull	-.58	1.13	.32	76	18.5	46	46
	6	Push-pull	-.17	.88	.52	210	16.0	10	10
	7	Push-pull	-.18	.85	.52	218	15.0	20	20
	8	Push-pull	-.21	.80	.52	228	14.5	30	30
	9	Push-pull	-.21	.83	.52	223	15.3	40	40
	10	Push-pull	-.15	.78	.53	233	15.0	50	50
	11	Push-pull	-.15	.82	.53	238	15.0	59	59
	12	Push-pull	-.20	.80	.51	213	15.0	46	Feathered
	13	Push-pull	-.21	.77	.51	218	15.0	Feathered	46
	14	Turn	.30	.89	.52	208	15.8	20	20
	15	Turn	.24	.88	.52	218	15.3	40	40
	16	Turn	.24	.89	.51	215	15.7	60	60
	17	Turn	.28	1.00	.41	127	17.0	46	46
	18	Turn	.64	1.21	.31	66	19.0	46	46
	19	Turn	.24	.57	.67	355	15.0	46	46
	20	Turn	.10	.67	.61	311	14.5	46	46
	21	Turn	.20	.48	.71	402	15.5	46	46
	22	Turn	.17	.81	.51	200	17.0	46	46

TABLE III.- SUMMARY OF FLIGHT TEST CONDITIONS FOR THE F-82 AIRPLANE - Concluded

Flight	Run	Maneuver	$C_{N_{WF}}$		Mach number	Dynamic pressure, lb/ft^2	Pressure altitude, ft	Engine manifold pressure, in.	
			Min.	Max.				Left	Right
5	1	Push-pull	0.00	0.54	0.70	426	14.0×10^3	58	58
	2	Push-pull	-.08	.78	.61	301	15.0	55	55
	3	Push-pull	-.25	.90	.50	191	17.0	52	52
	4	Push-pull	-.26	.92	.41	130	17.5	20	20
	5	Push-pull	.47	1.14	.31	74	17.5	20	20
	6	Push-pull	-.04	.57	.67	368	15.0	55	55
	7	Turn	.47	.88	.50	201	16.0	10	10
	8	Turn	.20	.88	.51	213	15.0	30	30
	9	Turn	.19	.90	.51	213	15.0	50	50
	10	Push-pull	-.12	.85	.51	225	14.5	20	20
	11	Push-pull	-.14	.87	.51	218	14.3	40	40
	12	Push-pull	-.14	.81	.52	223	14.8	60	60
	13	Push-pull	-.13	.90	.51	206	15.7	46	Feathered
	14	Turn	.31	.90	.51	225	14.0	46	Feathered
	15	Push-pull	-.60	1.25	.31	74	16.8	30	30
	16	Push-pull	-.45	1.05	.41	135	16.5	30	30

TABLE IV.- ESTIMATED MAXIMUM ERRORS IN PRINCIPAL MEASURED AND EVALUATED QUANTITIES

Quantity	B-45	F-82
M	0.01	0.02
q, lb/ft^2	5	5
n, g units	0.03	0.05
$dC_{N_C}/dC_{N_{WF}}$:		
Inner wing	-------	0.02
Outer wing	0.015	0.02
Fuselage	0.03	0.03
L_{c_o}:		
Inner wing, lb	-------	400
Outer wing, lb	500	300
Fuselage, lb	1,200	600
dBM/dS_a:		
Inner station, in.	-------	5
Outer station, in.	4	3
BM_o:		
Inner station, in-lb	-------	80,000
Outer station, in-lb	100,000	40,000

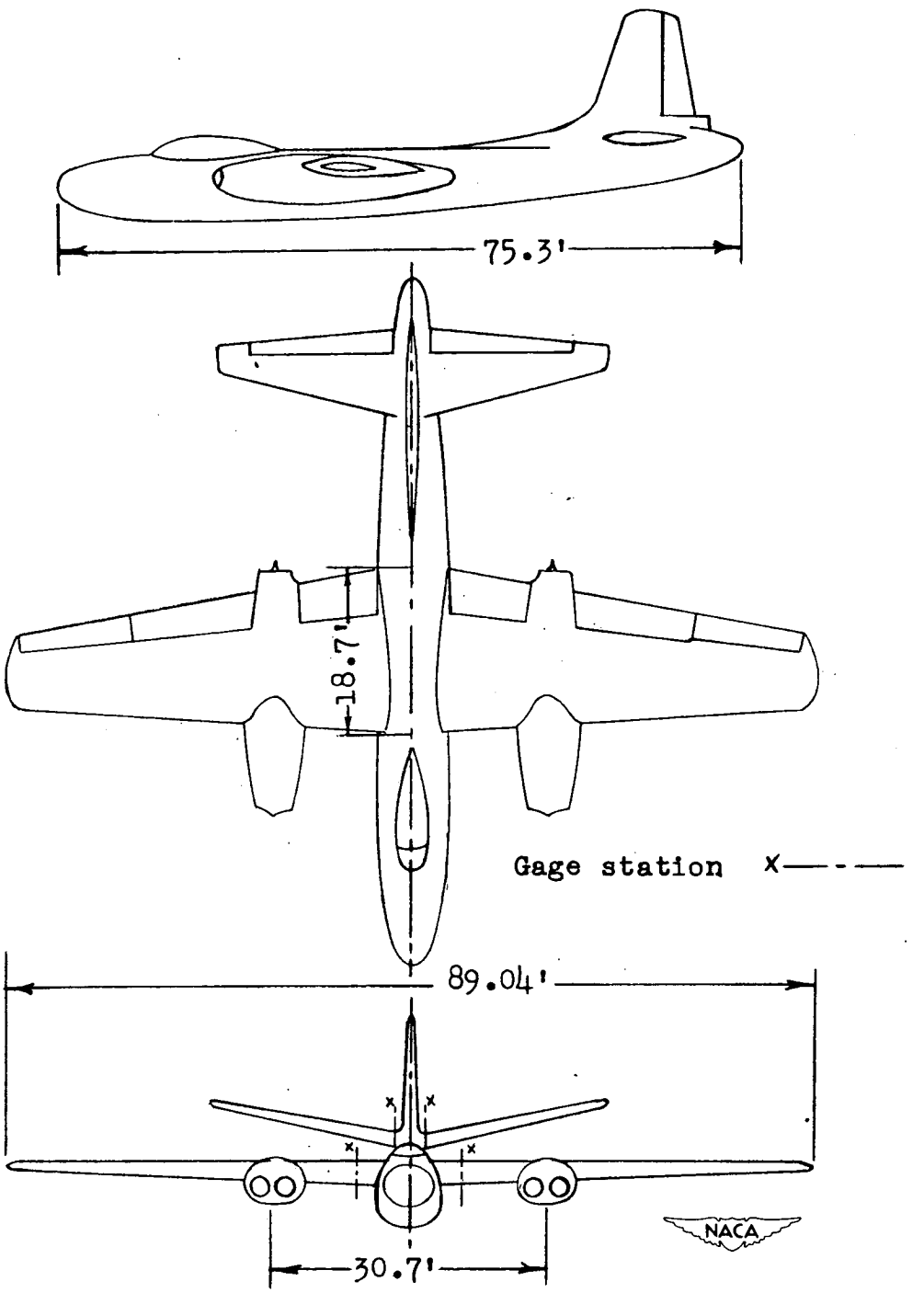

Figure 1.- Three-view drawing of the North American B-45 airplane.

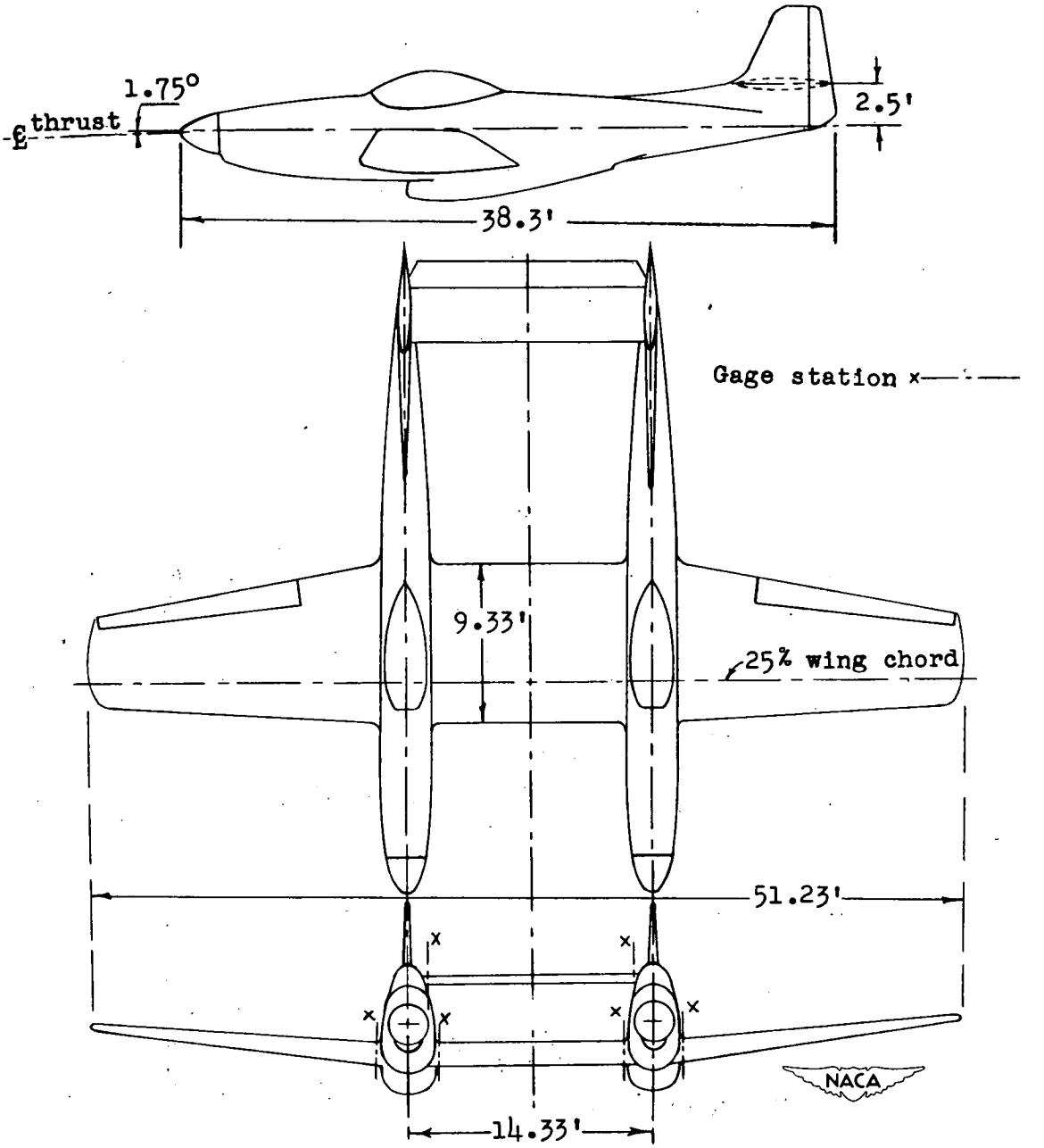

Figure 2.- Three-view drawing of the North American F-82 airplane.

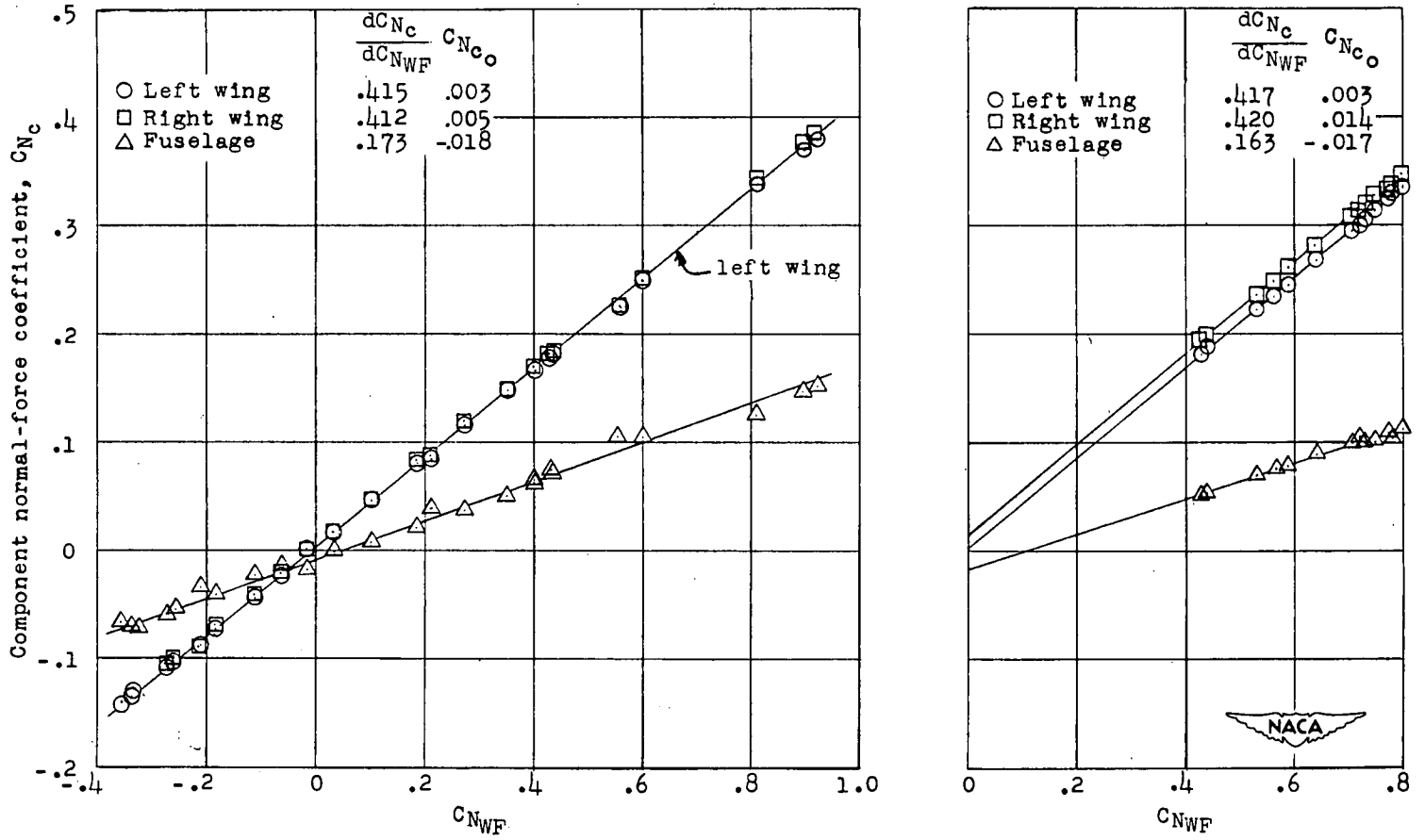

(a) Push-pull maneuver (Flight 18, Run 13).

(b) Turning maneuver (Flight 11, Run 5).

Figure 3.- Variation of component normal-force coefficients with wing-fuselage normal-force coefficient during typical maneuvers of the B-45 airplane.

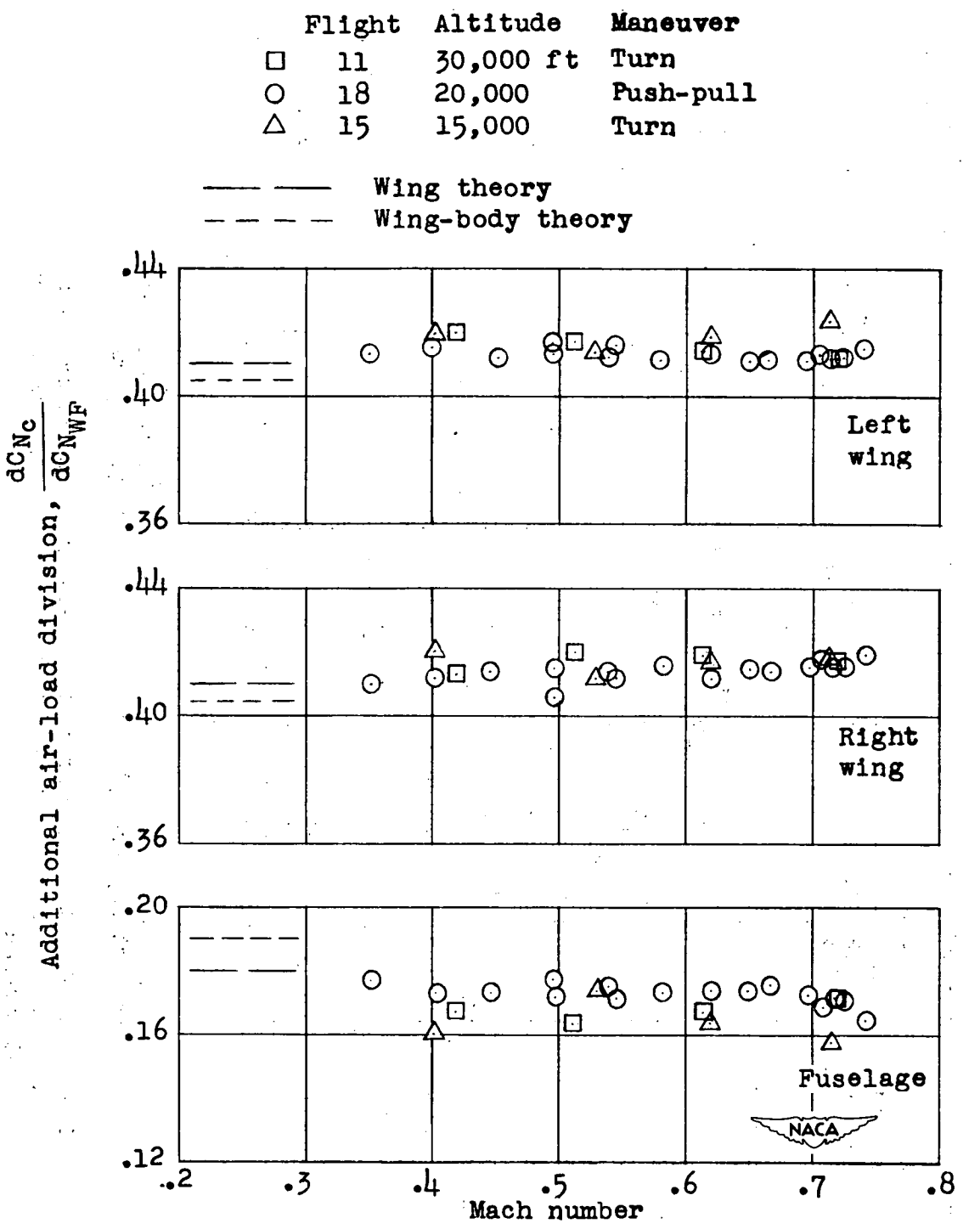

Figure 4.- Variation at several altitudes of additional air-load division with Mach number for the B-45 airplane.

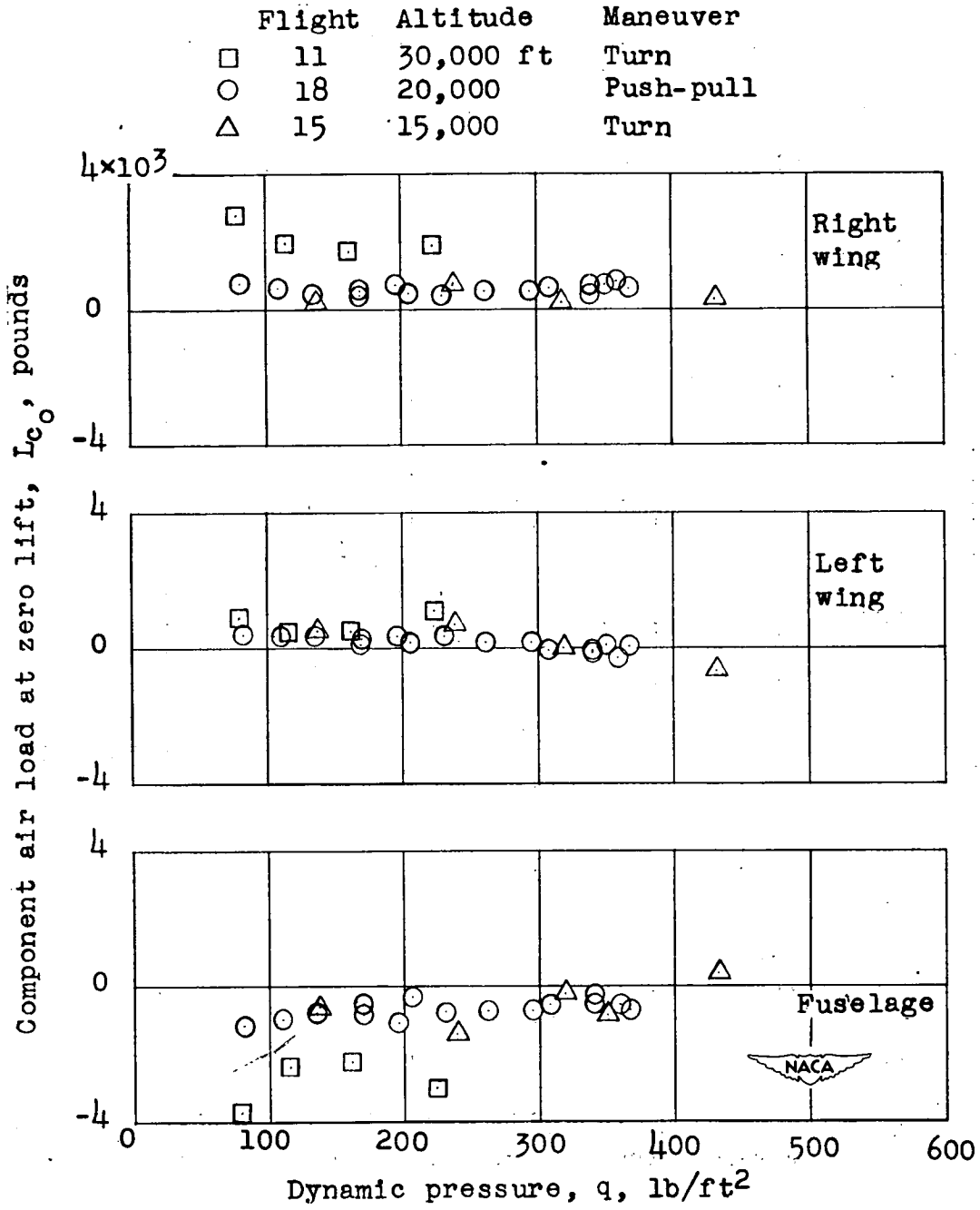

Figure 5.- Variation at several altitudes of component air load at zero lift with dynamic pressure for the B-45 airplane.

	Flight	Run	Maneuver	dBM/dS_a	BM_o
○	18	13	Push-pull	189.8	315,000
□	13	4	Turn	193.3	405,000

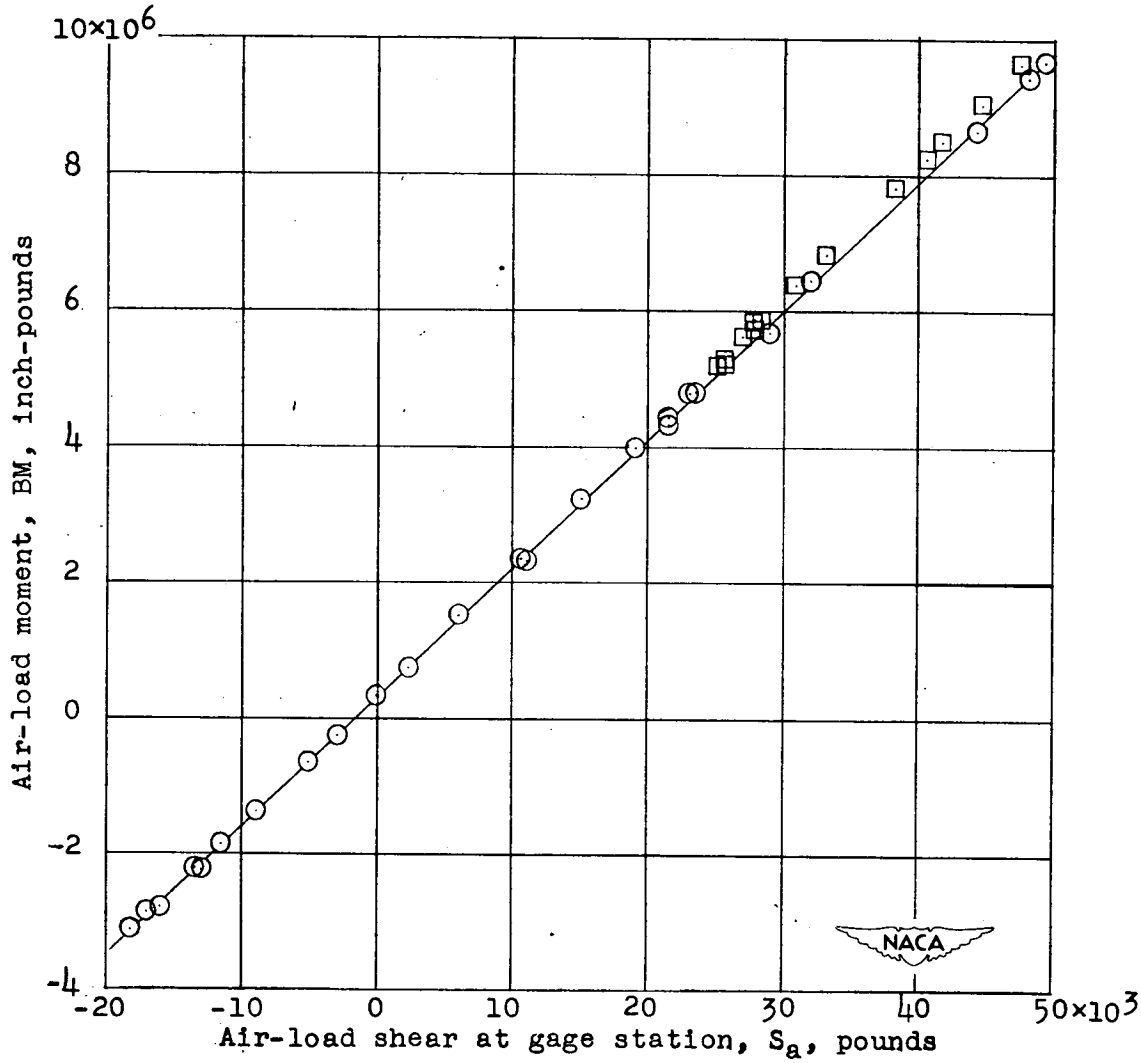

Figure 6.- Variation of aerodynamic bending moment with aerodynamic shear on the right wing of the B-45 airplane during typical maneuvers.

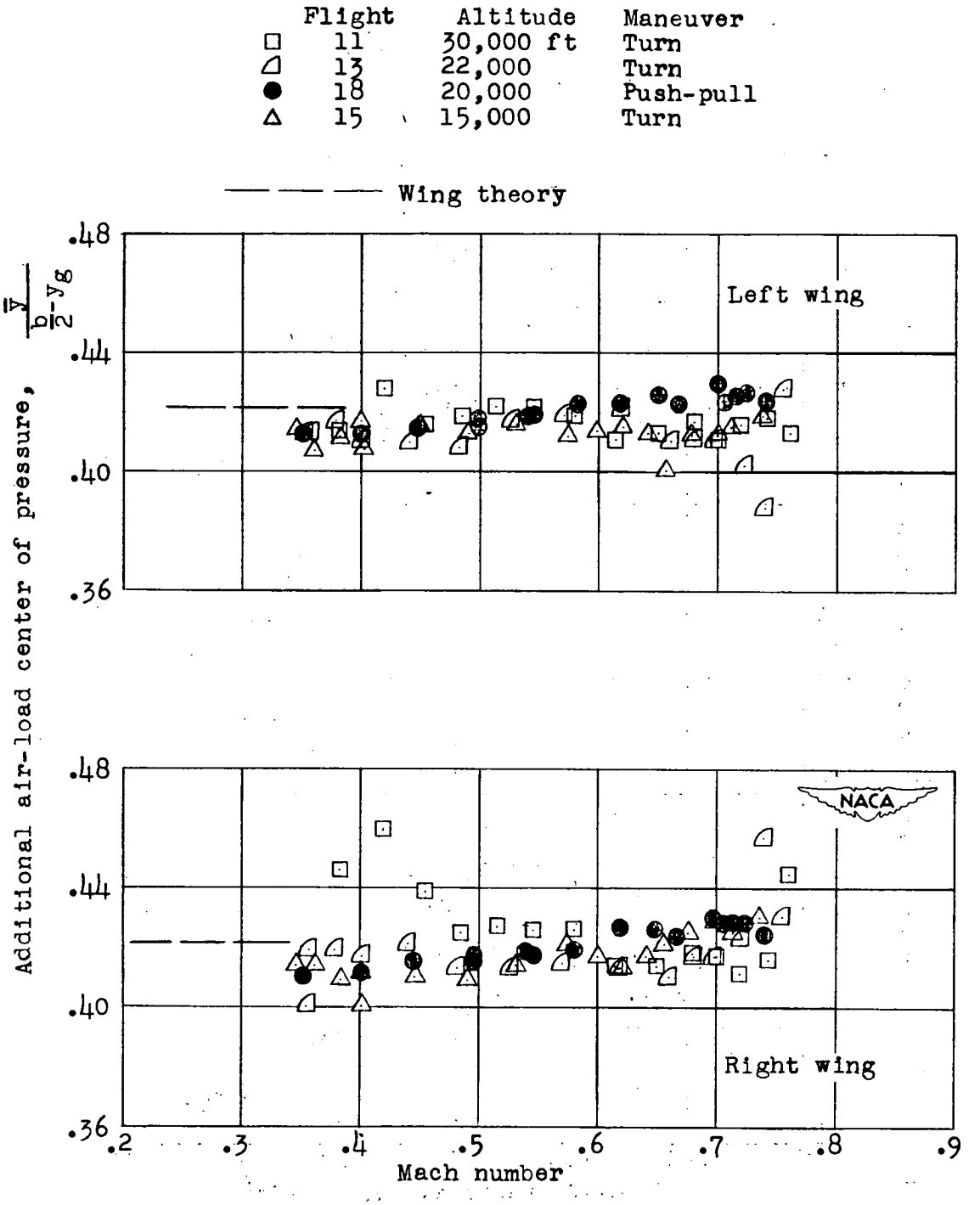

Figure 7.- Variation with Mach number at several altitudes of additional air-load centers of pressure outboard of wing gage stations on the B-45 airplane.

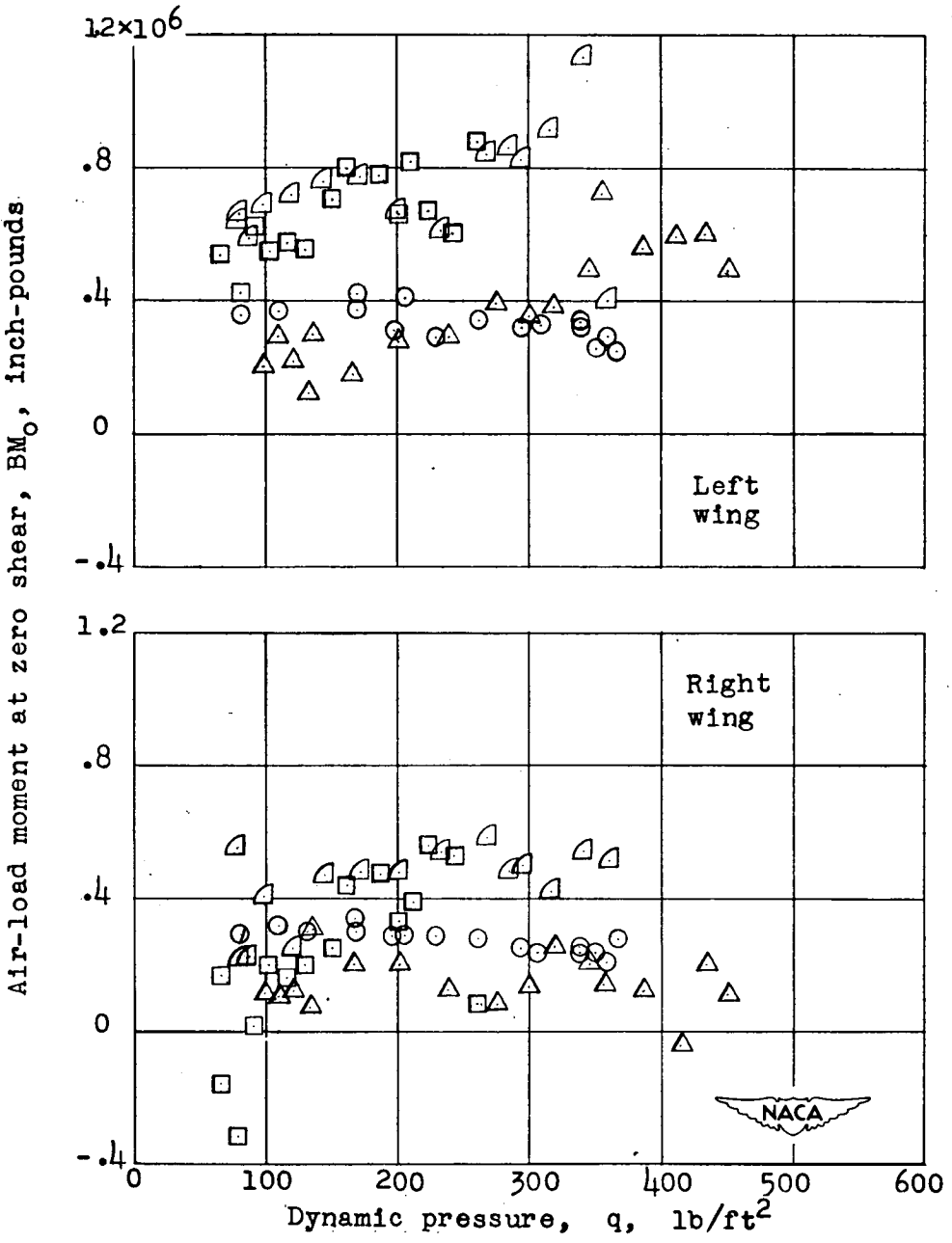

Figure 8.- Variation with dynamic pressure at several altitudes of air-load moment at zero air-load shear for each wing gage station on the B-45 airplane.

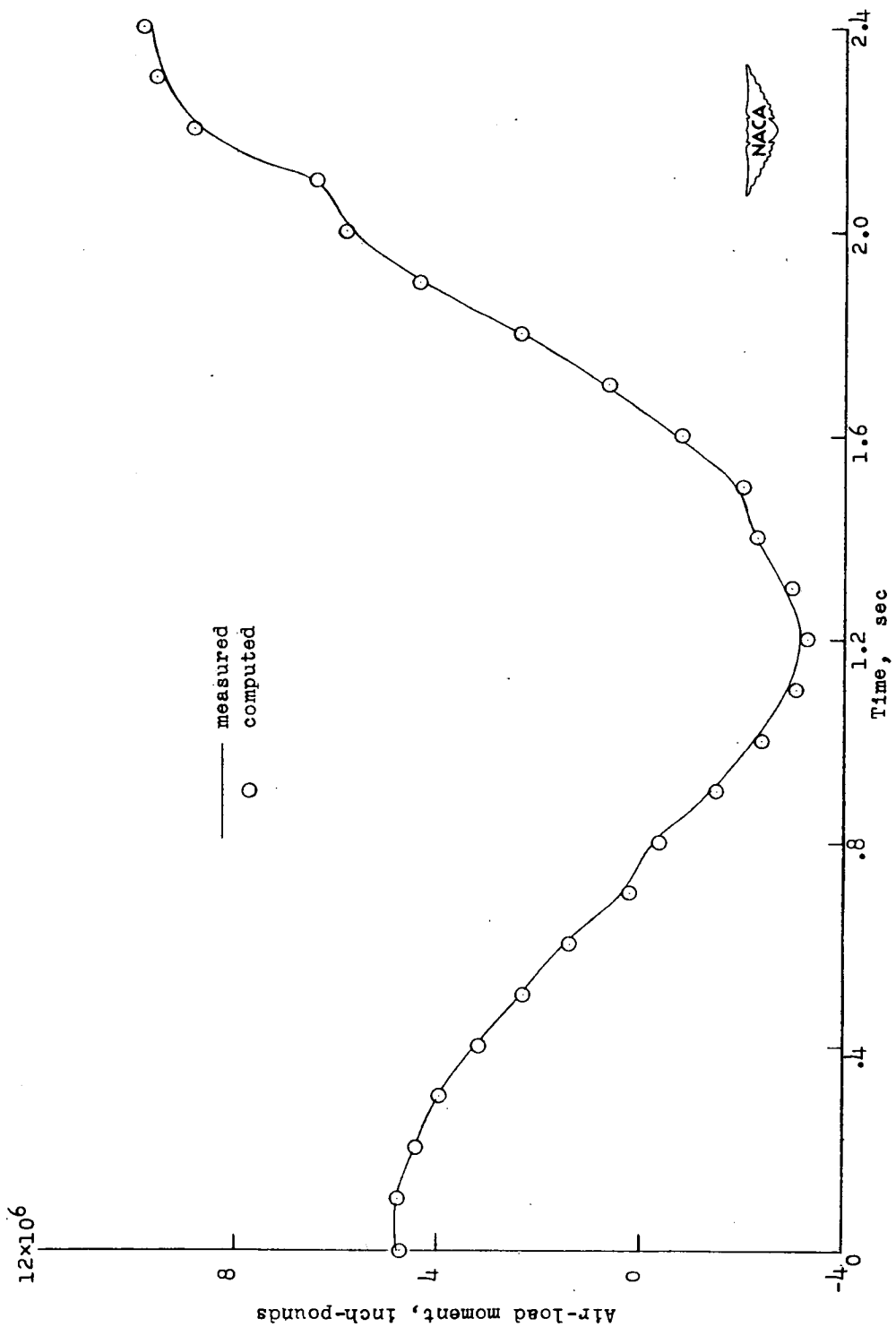

Figure 9.- Comparison of time variation of measured right-wing air-load moment with moment computed by equation (7) for the B-45 airplane during flight 18, run 13.

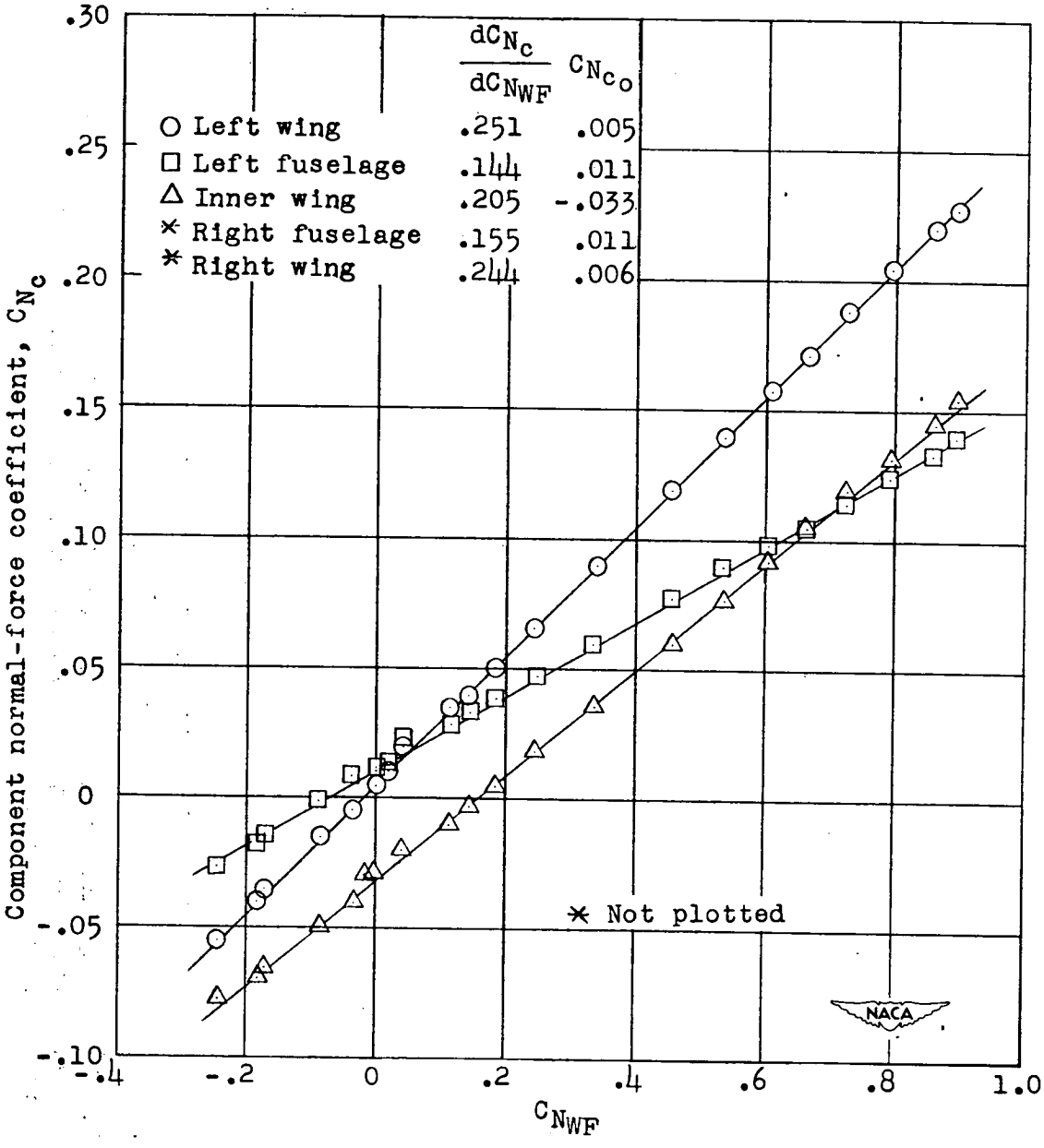

Figure 10.- Variation of component normal-force coefficients with wing-fuselage normal-force coefficient during a typical maneuver of the F-82 airplane. Flight 5, run 3.

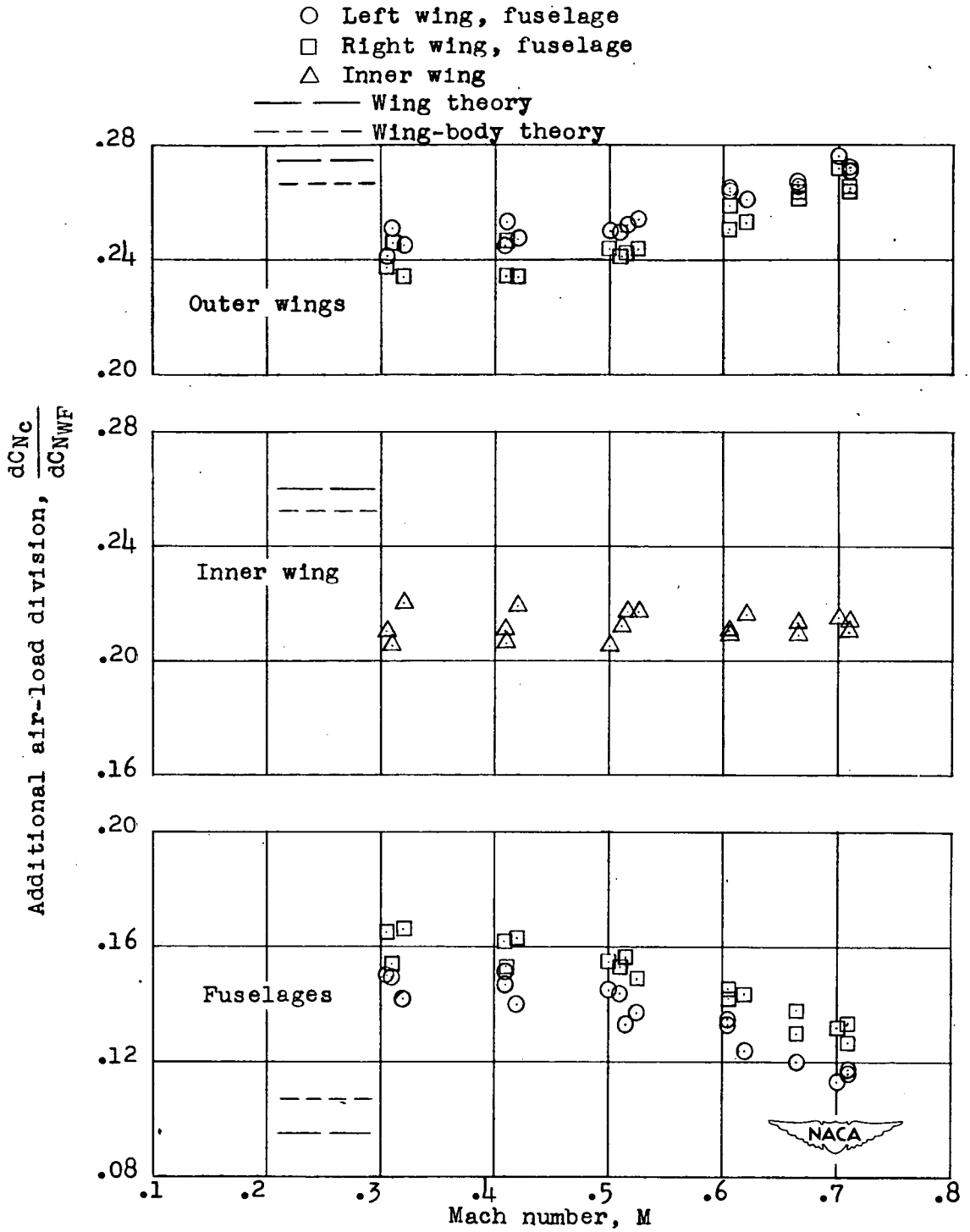

Figure 11.- Variation of additional air-load division with Mach number for the F-82 airplane.

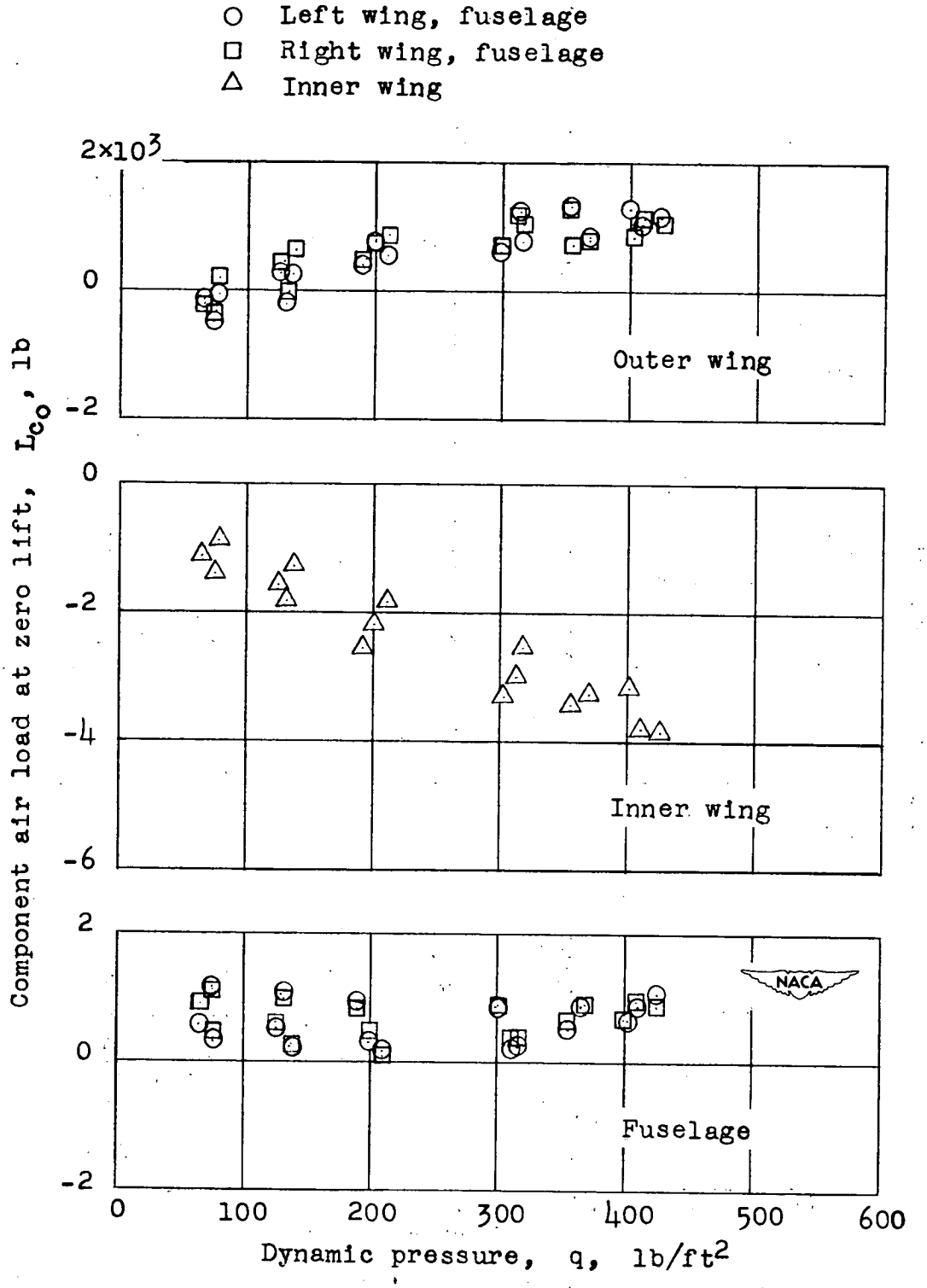

Figure 12.- Variation of component air loads at zero wing-fuselage lift with dynamic pressure during tests of the F-82 airplane.

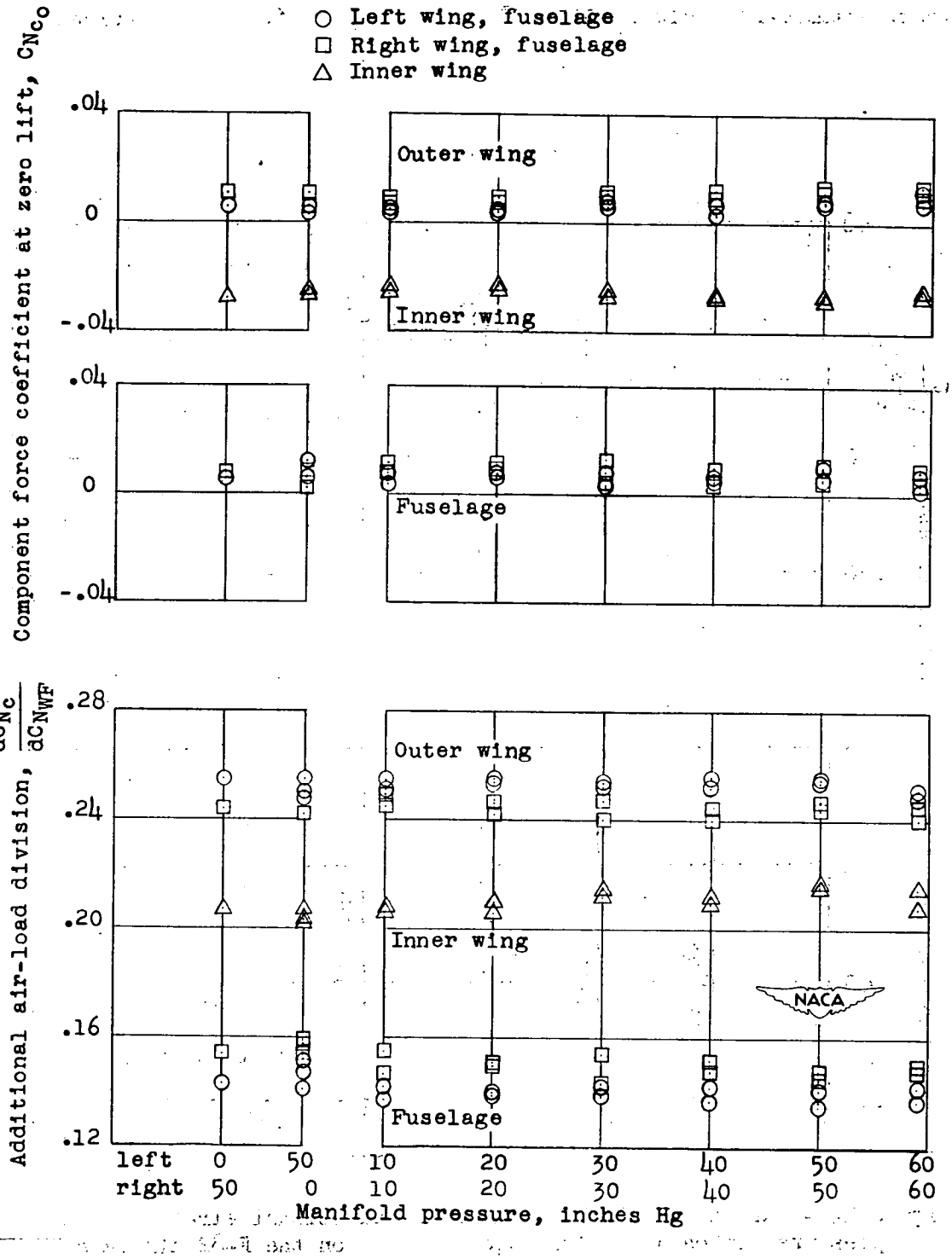

Figure 13.- Effect of power on the division of air load among the components of the F-82 airplane during flight.

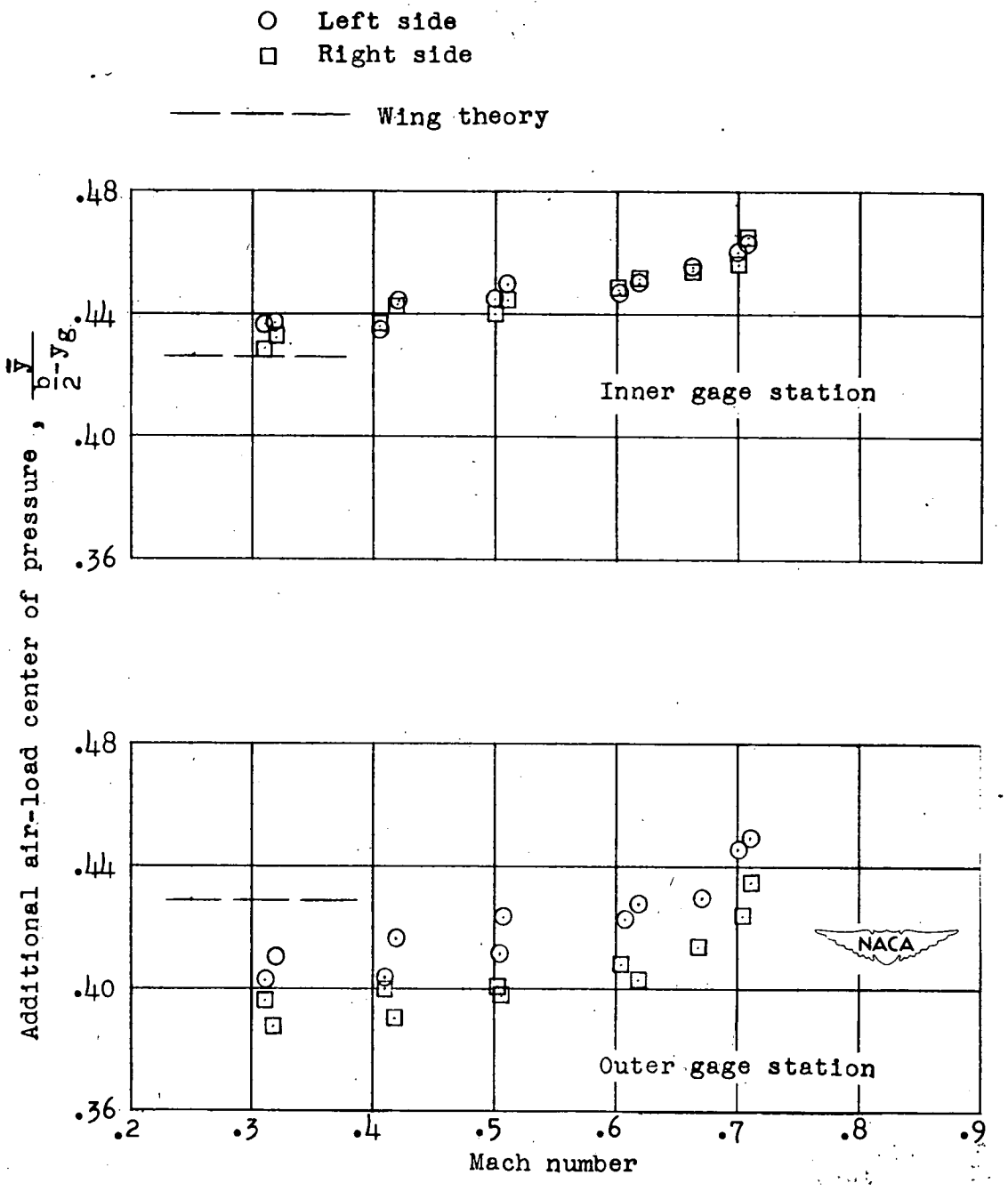

Figure 14.- Variation with Mach number of additional air-load centers of pressure outboard of wing gage stations on the F-82 airplane.

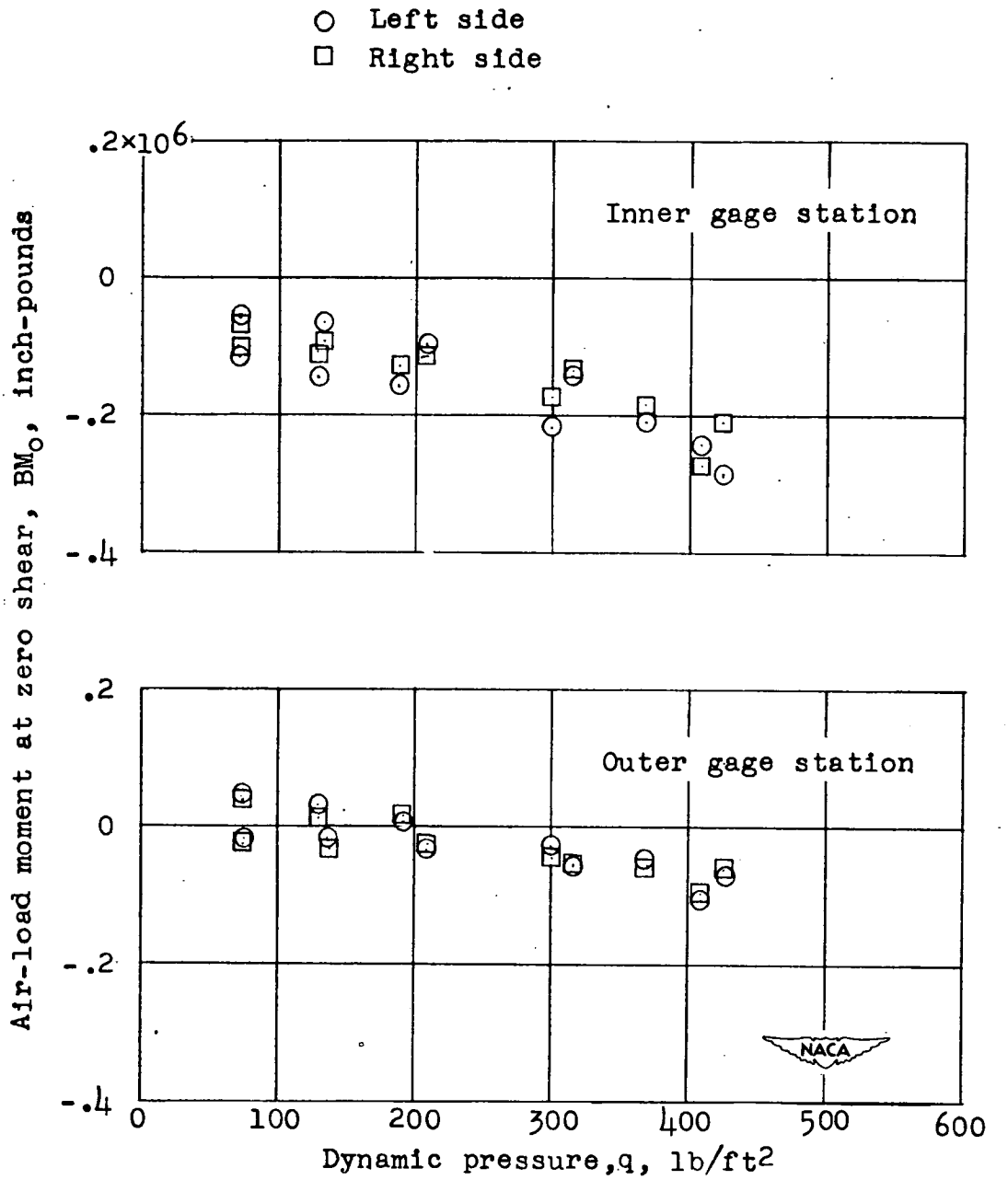

Figure 15.- Variation with dynamic pressure of air-load moment at zero air-load shear for each wing gage station on the F-82 airplane.